



Lawrence Berkeley Laboratory

UNIVERSITY OF CALIFORNIA

Physics Division

Mathematics Department

To be submitted for publication

Constrained Random Walks and Vortex Filaments in Turbulence Theory

A.J. Chorin

August 1989

For Reference

Not to be taken from this room



DISCLAIMER

This document was prepared as an account of work sponsored by the United States Government. While this document is believed to contain correct information, neither the United States Government nor any agency thereof, nor the Regents of the University of California, nor any of their employees, makes any warranty, express or implied, or assumes any legal responsibility for the accuracy, completeness, or usefulness of any information, apparatus, product, or process disclosed, or represents that its use would not infringe privately owned rights. Reference herein to any specific commercial product, process, or service by its trade name, trademark, manufacturer, or otherwise, does not necessarily constitute or imply its endorsement, recommendation, or favoring by the United States Government or any agency thereof, or the Regents of the University of California. The views and opinions of authors expressed herein do not necessarily state or reflect those of the United States Government or any agency thereof or the Regents of the University of California.

CONSTRAINED RANDOM WALKS AND VORTEX FILAMENTS IN
TURBULENCE THEORY*

Alexandre Joel Chorin

Department of Mathematics
University of California
and
Lawrence Berkeley Laboratory
Berkeley, California 94720

August 1989

* This work was supported in part by the Applied Mathematical Sciences Subprogram of the Office of Energy Research, U.S. Department of Energy, under Contract Number DE-AC03-76SF000098.

CONSTRAINED RANDOM WALKS AND VORTEX FILAMENTS IN TURBULENCE THEORY

Abstract

We consider a simplified model of vorticity configurations in the inertial range of turbulent flow, in which vortex filaments are viewed as random walks in thermal equilibrium subjected to the constraints of helicity and energy conservation. The model is simple enough so that its properties can be investigated by a relatively straightforward Monte-Carlo method: a pivot algorithm with Metropolis weighting. Reasonable values are obtained for the intermittency dimension D , a Kolmogorov-like exponent γ , and higher moments of the velocity derivatives. Qualitative conclusions are drawn regarding the origin of non-gaussian velocity statistics and regarding analogies with polymers and with systems near a critical point.

Introduction

Three dimensional incompressible flow can be approximated by following the evolution of a collection of vortex tubes, and discretizations that consider finite collections of tubes lead to vortex approximations [2],[4],[7],[18],[21]. One can consider the finite approximations as models of the Navier-Stokes equations and examine their statistical properties in the hope of gaining an understanding of turbulence. One must of course be aware that the properties of finite systems do not necessarily survive the passage to the limit of a continuous system. In particular, the finite systems greatly simplify the geometric complexity of the microstructures that occur in real turbulence.

The inertial range of scales in turbulent motion is the range of scales intermediate between the scales on which the fluid is stirred and the scales on which its energy is dissipated. These scales play a key role in the dynamics of turbulence. In the inertial range, turbulent flow can be viewed as being in approximate thermal equilibrium. If one represents the flow on these scales by a collection of vortex tubes, one can appeal to methods of analysis adapted from other branches of statistical mechanics [10],[11],[13]. The analyses and the calculations in earlier work along these lines are quite difficult. In the present paper we present simplified models of vortex configurations in the inertial range, simple enough so that their properties can be examined by relatively simple mathematical tools and also so that the results are easy to interpret. The price of relative simplicity is of course a certain unfaithfulness to the true equations of motion.

We shall replace the vortex tubes by vortex filaments, i.e., tubes with point cross-section. Various issues that have to do with the shape of the cross-section are thus avoided, but a major mechanism responsible for the formation of an inertial range is removed. The filaments are assumed to form a suspension sufficiently dilute so that the spectrum for large wave numbers can be determined by the properties of one of them. The filaments are supposed to be random walks in space, subjected to two constraints: self avoidance (which implies in particular a fixed helicity) and a weak form of energy conservation. The filaments are studied by a simulation on a lattice (thus removing one form of intermittency [10]); they are generated by a combination of a pivot algorithm [22],[25] and Metropolis sampling [5]. The model will be justified heuristically.

Even though the model is simple and the numerical method used to investigate it straightforward, the amount of computer time needed to complete the calculations is formidable, and the results are not complete. The reason for the large amount of labor emerges as one of the qualitative conclusions from the model. The results obtained are consistent with earlier results and conjectures. The model shows how global conservation properties can produce an inertial range, and provides a heuristic explanation for the appearance of non-gaussian velocity statistics. The vorticity (intermittency) dimension D is in acceptable agreement with earlier results (but one must be careful to notice that it is defined differently here than in earlier calculations). The inertial exponent γ that characterizes the energy spectrum is as close to what one knows as the model allows. Analogies with polymer systems and with critical phenomena appear naturally. In particular, support is given to the notion that as the viscosity tends to zero, a turbulent flow approaches a critical point. This observation explains the difficulty in extracting information about inertial exponents from numerical calculations; the inertial exponent is a critical exponent and as such is difficult to calculate.

The qualitative behavior of the model supports the conjectures made in [7],[8],[9], that the inertial range properties are due to the appearance of folded vortex tubes, which behave on large scales as self-avoiding walks, and on small scales contain a large number of folds (= "hairpins") that are needed to satisfy the constraint of energy conservation.

The rest of the paper is divided into the following sections: vortex methods; vortex folding; some scaling properties of fluid turbulence; polymers, self-avoiding walks and the pivot algorithm; simple models of folded vortex tubes; properties of the filament models; numerical results; and conclusions.

Vortex motion

The equations of motion of an ideal incompressible fluid in three space dimensions are

$$\frac{D\underline{\xi}}{Dt} = -(\underline{\xi} \cdot \nabla)\underline{u} \quad (1a)$$

$$\text{div } \underline{u} = 0, \quad \underline{\xi} = \text{curl } \underline{u}, \quad (1b, 1c)$$

where D/Dt is the material derivative, ∇ is the differentiation vector, \underline{u} is the velocity,

and $\underline{\xi}$ is the vorticity. We shall consider a flow without boundaries, and assume that initial conditions $\underline{\xi}(t=0)$ are available when needed. Equations (1b,1c) can be solved for \underline{u} and yield

$$\underline{u} = K * \underline{\xi} \quad (2)$$

where $*$ denotes a convolution and K is the matrix kernel

$$K = \frac{-1}{4\pi r^2} \begin{pmatrix} 0 & -x_3 & -x_2 \\ x_3 & 0 & -x_1 \\ x_2 & x_1 & 0 \end{pmatrix},$$

where $\underline{r} = (x_1, x_2, x_3)$ is the position vector and $r = |\underline{r}|$. Equation (2) is known as the Biot-Savart formula. Equations (1) have the following Lagrangean representation:

$$\frac{d\underline{x}}{dt} = \underline{u} = K * \underline{\xi}, \quad (3a)$$

where \underline{x} is a point moving with the fluid and \underline{u} is the velocity at \underline{x} . Equation (3a) is supplemented by the constraints

$$\text{div } \underline{\xi} = 0, \quad \int_{\Sigma} \underline{\xi} \cdot d\underline{\Sigma} = \text{constant (in space and time)} \quad (3b, 3c)$$

where Σ is a cross-section of a "vortex tube", i.e., a set of integral lines of $\underline{\xi}$ issuing from a closed curve nowhere tangent to $\underline{\xi}$. Equation (3a) states that $\underline{\xi}$ moves with the flow, and equations (3b,3c) express the conservation of angular momentum in a flow of constant entropy. If the flow is viscous rather than ideal, a Laplacian of $\underline{\xi}$ must be added to equation (1a) and a noise term to equation (3a). (For details, see e.g. [14].)

It is a well known fact that in turbulent flow vortex tubes stretch [2],[13]. As a result, the "enstrophy" $Z \equiv \int |\underline{\xi}|^2 d\underline{x}$ increases, possibly to infinity in a finite time [6],[7]. In general, $dZ/dt > 0$. The energy E of the flow can be written as

$$E \equiv \frac{1}{2} \int |\underline{u}|^2 d\underline{x} = \frac{1}{8\pi} \int d\underline{x} \int d\underline{x}' \frac{\underline{\xi}(\underline{x}) \cdot \underline{\xi}(\underline{x}')}{|\underline{x} - \underline{x}'|}. \quad (4)$$

The last expression is the "Lamb integral" [23]. We must have $dE/dt \leq 0$ in the absence of a stirring force. An additional invariant is the helicity $H = \int \underline{\xi} \cdot \underline{u} d\underline{x}$.

The problem of solving equations (3) is equivalent to the problem of solving equations (1) and is equally intractable. A more tractable problem is obtained by discretizing

equations (3): Consider a finite collection of vortex tubes of finite cross-section that approximate an initial vorticity distribution, and consider the motion of these tubes as defined by equations (3). To define the motion one has to make a decision as to the evolution of the cross-sections of the tubes. This is not a trivial matter, since the cross-sections can flatten or distort in various ways; here we want to make the simplest possible assumption and assume that the cross-sections of the tubes start out as circles and remain so; the radii of these circles can vary. One can show that the solutions of equations (1) can be approximated by a collection of vortex tubes with circular cross-sections [1],[3],[4],[7],[18] whose number must of course increase as the approximation is improved.

We consider the motion of a fixed number of such approximating vortex tubes. The statistical mechanics of such a collection of tubes is interesting because it sheds light on the behavior of numerical algorithms, and also because it constitutes a plausible cartoon of turbulence in which the great variety of micro-structures that appears in real fluid mechanics is replaced by the set of those structures that can be constructed from tubes of fixed circular cross-section. One cannot always claim that the results obtained from this model carry over to real turbulence as the number of tubes is increased; for example, spectral densities derived from discrete models do not necessarily survive a passage to the limit of a continuous vorticity distribution [13].

Vortex folding

We now present a heuristic analysis that explains why tubular vortices in a finite collection must fold. Consider a single long vortex tube V of unit circulation; V has a non-zero, small, circular cross section, with a radius that can vary along the tube. Suppose V can be approximately covered by N circular cylinders I_i , $i = 1, \dots, N$, of equal lengths ℓ and radii ρ_i , $i = 1, \dots, N$. The energy E can be approximated by \tilde{E} (see equation (4)):

$$8\pi\tilde{E} = \sum_i^N \sum_{\substack{j=1 \\ j \neq i}}^N \tilde{E}_{ij} + \sum_{i=1}^N \tilde{E}_{ii}$$

where

$$\tilde{E}_{ij} = \int_{I_i} d\mathbf{x} \int_{I_j} d\mathbf{x}' \frac{\underline{\xi}(\mathbf{x}) \cdot \underline{\xi}(\mathbf{x}')}{|\mathbf{x} - \mathbf{x}'|}.$$

Let \underline{t}_i be a vector lying along the axis of the cylinder I_i , originating at the center of I_i , of length $|\underline{t}_i| = \ell$, and pointing in the direction of $\underline{\xi}$ in I_i (assumed to be constant). If I_i and I_j are far from each other and $|i - j|$ is the distance between them, then

$$\tilde{E}_{ij} \simeq \frac{\underline{t}_i \cdot \underline{t}_j}{|i - j|}.$$

Assume this last relation holds approximately whenever $i \neq j$. If $i = j$, \tilde{E}_{ij} is a function of the radius ρ_i of I_i , $\tilde{E}_{ij} \rightarrow \infty$ as $\rho_i \rightarrow 0$ (for an analysis, see [10]). Thus

$$8\pi\tilde{E} \simeq \sum_i \sum_{j \neq i} \frac{\underline{t}_i \cdot \underline{t}_j}{|i - j|} + \sum_i \tilde{E}_{ii}(\rho_i) \quad (5)$$

with $d\tilde{E}_{ii}/d\rho_i < 0$. We shall call the double sum on the right hand side the “exchange energy” and the single sum the “self-energy”.

Suppose now that the tube V is stretched by the velocity field that includes the velocity field that it itself induces, in such a way that its volume is preserved. Suppose that the support of the new stretched tube V can still be approximated by a collection of cylinders of lengths ℓ ; their number N' will be larger than N , and most of their cross sections will be smaller than before. Thus the sum $\sum \tilde{E}_{ii}$ will increase because it will have more and larger entries. As the radii tend to zero, this sum will diverge. If \tilde{E} , the total energy, remains bounded, then the double sum over i, j must decrease, i.e., the tube must fold. Thus the vortex segments I_i arrange themselves in such a way that they shield the incipient singularity due to the singular Biot-Savart kernel. Note that this phenomenon has no analogue in two space dimensions, where there is no stretching and where “self-energies” can be safely subtracted from the total energy in defining a Hamiltonian.

A simple one-dimensional cartoon of equation (6) is:

$$\tilde{E} = \sum_{i=1}^N \sum_{\substack{j=1 \\ j \neq i}}^N t_i t_j \frac{1}{|i - j|} + \sum \tilde{E}_{ii}$$

where N is finite and fixed, the t_i are Ising-like spins, i.e., vectors that can point either up ($t_i = 1$) or down ($t_i = -1$), $|i - j|$ is the distance between the position of t_i and t_j , and \tilde{E}_{ii} is a function of a parameter ρ^{-1} that increases monotonically. Suppose the “spins”

are located at the nodes of a regular lattice, most of whose nodes are empty. The “spins” can move to empty locations or flip (i.e., change signs); ρ^{-1} increasing is interpreted as a stretching of the “spins”. In [9] a sequence of spin configurations is constructed, such that the “energy” \tilde{E} remains fixed. The \tilde{E}_{ii} increase, and thus the double sum must decrease; this requires the “spins” to bunch up as closely as possible on the lattice, with neighboring “spins” having opposite signs.

An interpretation of vortex folding in terms of capacity theory [16] can be found in [7],[8], and an analogy with the instability of the ground state of a collection of fermions to the formation of Cooper pairs can be found in [13].

A vortex tube cannot intersect itself as it evolves; this is a consequence of helicity conservation [26] and of the smoothness of the Euler flow map [19]; thus, to a first approximation, one can view a vortex tube as a non-self-intersecting tube folded so as to satisfy the constraint of energy conservation.

Some scaling properties of fluid turbulence

We now list some of the properties of turbulence in an incompressible fluid that we shall be studying with the model described below.

Consider a compact set Λ filled with fluid. The enstrophy in Λ is $Z_\Lambda = \int_\Lambda |\underline{\xi}|^2 d\underline{x}$. An ϵ -support of the vorticity is a set Λ_ϵ such that

$$\int_{\Lambda_\epsilon} |\underline{\xi}|^2 d\underline{x} \geq (1 - \epsilon) \int_\Lambda |\underline{\xi}|^2 d\underline{x},$$

i.e., a set that contains all but a fraction ϵ of Z . Suppose one can construct a smallest Λ_ϵ (up to negligibly small changes) for a given ϵ . Call it the ϵ -support of the vorticity and denote it also by Λ_ϵ . One can readily see that as a result of vortex stretching Λ_ϵ shrinks. It is consistent with the available numerical results and theory to assume that for t large enough the Hausdorff dimension D_ϵ of Λ_ϵ tends to a limit $D \neq 3$ as $\epsilon \rightarrow 0$. (For example, for the model problem $u_t + (u^2/2)_x = 0$, $\xi = u_x$, Λ_ϵ for $t > t_*$ and any $\epsilon < 1$ is the set of points where the shocks are located, with $t_* =$ time of formation of the first shock, and $D = 0$ for $t > t_*$.) D , if it is well defined, is a measure of the intermittency of the flow (for more details, see [7],[8],[10]).

An attempt was made in [7] to estimate D by extrapolation from a noisy initial value problem; it yielded the value $D \sim 2.5$. A more robust calculation [8] based on scaling arguments yielded a dimension ~ 2.35 for a set containing Λ_ϵ . Both calculations took into account in an essential way the changes in the non-zero cross-sections of the vortex tubes. An experimental study of the Hausdorff dimension of a vortex sheet in a turbulent flow [30] (not quite the same problem) yielded a similar value $D \sim 2.35$.

The energy spectrum $E(k)$ of homogeneous turbulence is calculated by the integration of the Fourier transform of the trace of the velocity correlation tensor over the sphere of radius $k = |\underline{k}|$, where \underline{k} is the wave vector dual to the separation \underline{r} . The mean energy at a point is $\int_0^\infty E(k)dk$. Similarly, the vorticity spectrum $Z(k)$ is calculated from the vorticity correlation function, and the equality $Z(k) = k^2 E(k)$ reflects the definition $\underline{\xi} = \text{curl } \underline{u}$ [2]. It is generally believed that in the inertial (= equilibrium) range $E(k) \sim k^{-\gamma}$ where γ is the inertial (Kolmogorov) exponent. A widely accepted value for γ is $\gamma = 5/3$. In some recent work it has been postulated that $\gamma = 5/3$ is a “mean-field” value and that intermittency corrections proportional to $(3 - D)$ are needed to account for the effect of fluctuations. It has been shown in [8],[10] that $\gamma = 5/3$ already takes into account the effects of intermittency and fluctuations; $\gamma = 5/3$ and $D < 3$ are fully compatible.

Polymers, self-avoiding walks and the pivot algorithm

We now present a short discussion of polymers and self-avoiding walks that will soon be connected with the preceding discussion of vortex tubes.

A polymer can be viewed as a long string of beads connected by rods, randomly placed in space, with arbitrary angles between the rods [17]. If $\langle r_N \rangle$ denotes the average distance between the first and the N -th bead, one expects $\langle r_N \rangle \sim N^\mu$ for large N , where μ is a characteristic exponent. In the simple model of a polymer that we just described one obtains $\mu = 1/2$ from the central limit theorem. If one requires that the polymer be self-avoiding, i.e., if one assumes that the beads have a finite volume and cannot simultaneously occupy the same location, then $\mu = \mu_0 =$ the Flory exponent. Intuitively, $\mu_0 > 1/2$; an elegant thermodynamic argument [17] yields $\mu_0 = 3/5$ (the Flory value) in three dimensional space. More generally, additional constraints on the polymer produce

different values of the exponent μ .

A polymer can be modelled as a random walk on a lattice. If the constraint of self-avoidance is not imposed, the random walk can be generated by a random walker who leaves the origin in a cubic lattice and at each step has an equal probability of stepping forth in each of the 6 available directions. We shall call such a walk a “free” walk. If the polymer is self-avoiding, the walker must be prevented from visiting the same location twice; the result is a self-avoiding walk on a lattice. At equilibrium one assumes that each possible self-avoiding walk of N steps has an equal probability of occurring. If $\langle r_N \rangle$ is the average end-to-end length of a self-avoiding walk with N steps, $\mu_0 \sim \log \langle r_N \rangle / \log N$ for large N . Numerical experiments with such walks corroborate the heuristic value $\mu_0 = 3/5$ [25].

Given the exponent μ , one can estimate the correlation function for the polymer [17]. Take a point on the polymer, there are on the average $N \sim r^{1/\mu}$ beads in a sphere of radius r centered at that point; there are $\sim r^{(1/\mu)-1}$ beads between r and $r + dr$; the bead density at a distance r is thus $\sim r^{(1/\mu)-1}/r^2 = r^{(1/\mu)-3}$, i.e., the correlation function for small r behaves as $r^{(1/\mu)-3}$ (r must be small to avoid corrections due to the finite length of the polymer and the possible presence of other polymer chains in the ambient medium). One can define the spectrum of the polymer as the Fourier transform of the correlation function; if k is the radial wave number, a simple calculation or even a dimensional analysis yields a spectrum $\sim k^{-1/\mu}$ for large k .

We will wish to make an analogy between polymers and vortex tubes and thus compare the polymer spectrum with the energy spectrum defined above. To obtain the analogue of the vorticity spectrum $Z(k)$ one has to average the polymer spectrum over a sphere of radius k , which adds a factor $\sim k^2$, and then to obtain an “energy” spectrum one has to divide by k^2 , and thus for a polymer $E(k) \sim k^{-1/\mu}$ for large k . In particular, for a self-avoiding polymer, $E(k) \sim k^{-5/3}$, and for a “free” polymer $E(k) \sim k^{-2}$.

Consider the center line of the polymer. Its Hausdorff dimension is $D = 1/\mu$, as can be read from the scaling relation $N = \langle r_N \rangle^{1/\mu}$. Thus $E(k) = k^{-\gamma}$, $\gamma = D$, where $\gamma = 1/\mu$. Thus, for a polymer, dimension and inertial exponent are related, with $d\gamma/dD = 1 > 0$ [11].

The problem of generating lattice self-avoiding walks on the computer in order to calculate μ is far from trivial. An effective algorithm for doing so is the pivot algorithm described in [25]. Consider the set of automorphisms of the cubic lattice; they can be represented by the set of matrices with columns g_i , $i = 1, 2, 3$, such that $g_i = \sigma_i \ell_{\pi(i)}$, where $\sigma_i = \pm 1$, $i = 1, 2, 3$, $\pi(i)$ is a permutation of $(1, 2, 3)$, and ℓ_j is the unit vector in the direction j . One can readily generate an algorithm that generates one of these matrices, with each matrix having an equal probability of being chosen.

To construct self-avoiding walks with N steps, start with a simple self-avoiding walk (for example, a straight line). Pick a point on that walk other than an end-point, with all points having an equal probability of being picked. Turn all the points to the right of the point picked by an automorphism chosen at random (“to the right” means “furthest from the first point as one travels along the chain”). Check if the resulting walk is self-avoiding. If it is, take it; if it is not, consider the preceding self-avoiding walk to be the next member of the sequence of walks; then repeat the procedure. In [25] it is shown that this algorithm produces a sequence of self-avoiding walks with the right probability distribution and with high efficiency ($O(N)$ operators for generating a new N -step random walk independent of the earlier ones in the sequence). Computational details and a description of the various precautions that must be taken are also contained in [25]. It should be mentioned that in particular a certain number of steps must be taken before the sample walks are used or else the result may be unduly influenced by the starting configuration. The exponent μ can be evaluated from the formula $\mu_0 = \log \langle r_N \rangle / \log N$. The error in μ_0 as a function of the number n of configurations over which one averages can be estimated as follows: suppose σ_N is a measure of the uncertainty in $\langle r_N \rangle$. Then an estimate of the statistical error in μ_0 is

$$e_N = \left| \frac{\log(\langle r_N \rangle + \sigma_N) / \log N - \log(\langle r_N \rangle - \sigma_N) / \log N}{\log N} \right|. \quad (6)$$

If the successive sample walks were statistically independent one could easily estimate σ_N . However, the sample walks are not independent. In fact, the limit $N \rightarrow \infty$ defines a critical point for self-avoiding walks and the achievement of independence is hampered by the phenomenon of critical slow-down [5]. If one estimates σ_N by the standard deviation, as

if the successive estimates were independent, the resulting value of e_N is an underestimate of the error. We shall not carry out an analysis of this situation. The reasons for this cavalier procedure will be described in due course. The fact that the limit $N \rightarrow \infty$ is a critical limit will be of significance for the final conclusions of this paper.

A simple model of folded vortex tubes

Our simplified model of an ensemble of vortex tubes will be an ensemble of self-avoiding walks, endowed with a direction so as to make the links in the walk into vectors, and subjected to a weak form of an energy conservation constraint patterned after equation (5).

It is important to note at the outset that by losing information about the structure of the vortex cores (and thus replacing the tubes by filaments) we lose a lot of information. The analysis in earlier work ([7],[8],[9]) relies heavily on a careful balancing of the energy increases due to the reduction in vortex cores during stretching and the energy decreases that result from folding. What will be displayed below is more a cartoon than a complete model. A careful analysis must be made of what information can be expected from such a model. However, the simplicity of the model leads to calculations that are conceptually simple and thus the result is informative.

It was shown above that the energy of a vortex system could be approximately divided into a self-energy (that cannot be evaluated without information about vortex cores) and an exchange energy defined by the double sum in equation (5). The analogue of that double sum from the filament on the lattice is

$$E = \sum_i \sum_{j \neq i} \frac{\underline{e}_i \cdot \underline{e}_j}{|i - j|} \quad (7)$$

where \underline{e}_i is a unit vector pointing in one of the six directions $(\pm 1, 0, 0)$, $(0, \pm 1, 0)$, $(0, 0, \pm 1)$, i is an index characterizing the location, and $|i - j|$ is the distance between the locations i and j (specifically, between the centers of the lattice links that issue from locations i and j). The length of the lattice links can be taken as 1 without loss of generality. By the time a vortex tube has become a filament the self-energy is large so the exchange energy E should be small. On the other hand various filaments can absorb and emit energy so

no specific bound can be placed on E . A reasonable version of energy conservation is one in which each self-avoiding vortex, i.e., an oriented self-avoiding walk, is assigned a statistical weight proportional to $\exp(-E/T)$, where E is given by (7) and T is a small “temperature”.

T is a measure of the uncertainty in the model. The total energy available to a filament depends on the other filaments and on the evolution of the self-energy, which is not taken into account because the cross-sections are not known. $T = \infty$ produces a self-avoiding filament. T very small may lead to a single realizable configuration that minimizes E . We wish to pick T small enough to have an effective energy constraint but not so small that there are no fluctuations. In effect, we have a one-parameter family of models, and we are interested in the models that correspond to the smaller values of T . In practice, T “small” will turn out to define the model adequately. To generate such energy-constrained, self-avoiding vortex filaments one need only modify slightly the pivot algorithm described above by a Metropolis rejection technique [5]: given a self-avoiding walk with energy $E = E_{old}$, generate another self-avoiding walk by the pivot algorithm, calculate its energy E_{new} , and accept this new walk with probability $p = \min\left[1, \exp(-(E_{old} - E_{new})/T)\right]$. If a new walk is not accepted, the previous walk is taken as the next in the sequence of realizations of the walk. The ergodicity and detailed balance conditions for the modified sampling follow trivially from those for the pivot algorithm.

All the energy constrained vortex filaments will be self-avoiding, and we shall refer to them simply as energy constrained filaments. One can endow both a free random walk and a self-avoiding walk with a direction and thus obtain a “free” vortex filament or a “self-avoiding” vortex filament. These will be used in the numerical work below.

One can reformulate the model as a free random walk weighted by a weight proportional to $e^{-H/T}$, where

$$H = \lim_{\epsilon \rightarrow 0} \sum_i \sum_j \phi_\epsilon(|i - j|) + E, \quad \lim_{\epsilon \rightarrow 0} \phi_\epsilon = \text{Dirac } \delta, \quad (8)$$

(for the generation of self-avoiding walks by means of ϕ_ϵ , see [24]).

The conjecture made in [8],[10] was that the equilibrium configuration of vortex filaments can be approximated by allowing vortex tubes to stretch subject only to the con-

straints of energy and helicity conservation. It was further conjectured that energy conservation creates folded tangles which affect the Hausdorff dimension of the support of the vorticity, and that the large scale behavior of vortex tubes was determined by the constraint of conservation of helicity, which is equivalent to self-avoidance. It was further conjectured that the effects of a vortex cross-section of finite capacity and of the vector nature of the vorticity conspire to create a spectrum with the same exponent as the self-avoiding walk, i.e., a Kolmogorov spectrum. We shall check some of these conjectures on our models, remarking that one important ingredient (a variable cross-section) is missing.

A discussion of hairpins that does not rely on a vortex representation can be found e.g. in [29].

Properties of the filament models

We now list various computable properties of the model, the values they can be expected to assume, and their relation to properties of real fluid turbulence.

The Hausdorff dimension D of the vortex filaments can be calculated as before: $D = 1/\mu$, $\mu = \lim_{N \rightarrow \infty} (\log \langle r_N \rangle / \log N)$. One should be very careful when one tries to identify this quality with the dimension D calculated, e.g., in [8], which is strongly dependent on the variation in the cross-section of tubes.

In the case of vortex filaments, it is no longer true that in $E(k) \sim k^{-\gamma}$ one has $\gamma = 1/\mu$, since the vector nature of the vorticity must be taken into account. Let $\underline{\xi}(\underline{r}) = (\xi_1(\underline{r}), \xi_2(\underline{r}), \xi_3(\underline{r}))$ be the vorticity at a position \underline{r} in physical space. The correlation between $\underline{\xi}(0)$ and $\underline{\xi}(\underline{r})$ is the average of $\sum_i \xi_i(0) \xi_i(\underline{r})$. Consider a sphere of radius $r = |\underline{r}|$, and the function

$$\phi(r) = \sum_{|\underline{r}'| \leq r} \sum_i \xi_i(0) \xi_i(\underline{r}').$$

Suppose $\phi(r)$ has the form $\phi(r) \sim r^{\mu'}$, $\mu' = \text{constant}$. An analysis that follows step-by-step the analysis of the correlation function and the spectrum in the polymer case yields $E(k) \sim k^{-\gamma}$ for large k with $\gamma = 1/\mu'$. Note that $\mu' \neq \mu$; the simple relation between γ and D in the polymer case is lost.

To estimate μ' , consider a vortex filament on a lattice, having N links, generated by

the algorithms described in the preceding section. Let $\underline{\xi}(j) = (\xi_1(j), \xi_2(j), \xi_3(j))$ be the vorticity vector at the location γ along the filament; $\underline{\xi}(j)$ points in one of six possible directions. For large N ,

$$\mu' = \log\langle r_N \rangle / \log\langle \phi_N \rangle,$$

where $\langle r_N \rangle$ is the average distance between the first and N -th links (say between their centers), and $\langle \phi_N \rangle$ is the average value of the sum

$$\phi_N = \sum_{j=1}^N \sum_{i=1}^3 \xi_i(j) \xi_i(j_0), \quad j_0 \text{ fixed.}$$

ϕ_N replaces the N of the scalar formula for μ . Note that ϕ_N is simply the scalar product of $\sum \underline{\xi}(j)$ with a $\underline{\xi}$ at a fixed location; to avoid edge effects, i.e., to avoid the consequences of the fact that the constraint of self-avoidance and energy conservation are less restrictive at the ends of a finite filament than in the middle, pick j_0 far from the ends (e.g., in the middle). An error estimate for μ' can be obtained by the obvious generalization of (6):

$$e_N = \left| \log(\langle r_N \rangle + \sigma_N) / \log(\langle \phi_N - \sigma'_N \rangle) - (\log(\langle r_N \rangle - \sigma_N) / \log(\langle r_N \rangle + \sigma'_N)) \right| \quad (9)$$

where σ_N, σ'_N are estimates of the uncertainties in $\langle r_N \rangle, \langle \phi_N \rangle$, respectively. A crude estimate of e_N can be obtained by calculating σ_N, σ'_N as if the successive estimates of r_N, ϕ_N were independent.

Note that $\phi_N \leq r_N$, and thus $\mu' \geq 1, \gamma \leq 1$. These inequalities remind us forcefully that the filament model is unrealistic; the cross section of vortex tubes has an important role. In particular, an unstretched vortex configuration is a straight line, and thus $\mu' = 1, \gamma = 1$, while for an unstretched vortex configuration in a real fluid $\gamma > 3$ (the condition that $Z(k)$, the vorticity spectrum, be integrable and thus $\underline{\xi}$, the vorticity field, be locally in L_2). A local cascade non-intermittent model yields $\gamma = 2$ (see [10]); the discrepancy between these models is a reflection of the drastic and unrealistic assumptions in local cascade models. Note furthermore that a spectrum with $\gamma \leq 1$ has an infinite energy density (as indeed it should with vortex filaments carrying the vorticity). The implications of these facts for numerical computation are discussed in the concluding section of this paper.

To see what the computed values of μ' and $\gamma = 1/\mu'$ in the model can tell us about real flow, consider a few simple situations. As was already stated above, for an unstretched

filament $\mu' = 1, \gamma = 1$. If the vortex filament is free, the orientations of the vortex segments are uncorrelated, $\mu' = \infty, \gamma = 0$ (this situation was already discussed in [11]). μ' thus measures the amount of disorder in the systems. If the turbulence spectrum is created by the constraints, one should expect $1 < \mu' < \infty, 0 < \gamma < 1$, corresponding qualitatively to the inequalities for the Kolmogorov exponent $\gamma_0 = 5/3: 0 < \gamma_0 < 3, 0 < \gamma_0 < 2$ that yield a value of γ intermediate between 0 and the value that corresponds to a non-turbulent medium.

Note that in the model $d\gamma/dD < 0$, the opposite situation from the polymer case; however, for a fluid $d\gamma/dD > 0$, since as D increases in the model, the corresponding fluid vortex is more stretched, and thus the support of the enstrophy is smaller. Another manifestation of this discrepancy between reality and our model is that in a fluid that starts from rest the value of D decreases to its equilibrium value [7], while here the value of D will increase to its equilibrium value.

Given a vortex filament, the velocity field at a point \underline{x} in space is obtained by a discrete form of the Biot-Savart law (2):

$$u(\underline{x}) = \sum_j K(\underline{x} - \underline{x}_j) \xi_j, \quad (10)$$

where the sum is over the filaments, \underline{x}_j is the center of the j -th link and $\underline{\xi}_j$ is its vorticity vector. This formula can be differentiated to yield derivatives of \underline{u} .

Given a random variable η with mean 0, its skewness S and flatness F are defined as $S = \langle \eta^3 \rangle / \langle \eta^2 \rangle^{3/2}$, $F = \langle \eta^4 \rangle / \langle \eta^2 \rangle^2$, where the brackets denote averages. We shall be calculating below the skewness and flatness of the derivatives of u . For a gaussian variable, $S = 0, F = 3$. Note that even for a free filament, the components of the velocity vector cannot be gaussian. For a free filament, the large N limit of (10) behaves like

$$\int K(\underline{x} - \underline{w}) d\underline{w}$$

where \underline{w} is vector valued Brownian motion. Such integrals have been analyzed in [27],[28] for the simpler case of scalar w and a kernel in L_2 , and the result is not gaussian; such integrals are not mere sums of independent variables to which the central limit theorem applies. The Biot-Savart kernel produces a non-gaussian velocity field. Note however that

the skewness of the velocity derivatives should, in our model, be zero; that skewness is a measure of energy transport across scales [2] and thus should be zero at equilibrium. To evaluate that skewness in an equilibrium model one needs either a Kubo formula [15] or a model of hairpin formation and removal [12] that is beyond the resolution of the present model.

Numerical results

We shall now display numerical results from calculations with free, self-avoiding and constrained filaments. In each case, N , the number of links in the filament and n , the number of realizations of the filament, are numerical parameters. In the constrained case T , the “temperature”, is an additional parameter. In the case of a free filament, each realization can be generated from scratch by allowing a random walker to perform N steps on a lattice, and successive realizations are independent.

(a) **Results for free filaments.** These are included as a check on the validity of the overall procedure. A detailed convergence study as a function of N and n will not be displayed in this case. With $N = 801$, $n = 10^5$ we obtain $\mu = .488 \pm 4 \times 10^{-3}$ (the error estimate is simply the standard deviation of the estimate). The exact value is of course $\mu = .5$. The corresponding computed dimension is $D = 2.049 \pm 0.016$ (the exact value is $D = 2$). The calculated value of μ' is $\mu' = 96 \pm ?$, where ? denotes the fact that the estimate (6) is indefinite, one of the arguments of the logarithms being negative. The exact value is $\mu' = \infty$. The corresponding computed value of γ is $\gamma = 0.01 \pm ?$, the exact value being $\gamma = 0$.

The skewness of $\partial u / \partial x$ calculated at the mid-point of the filament, is $S = -0.037 \pm 0.076$, an estimate quite compatible with $S = 0$. The flatness F of $\partial u / \partial x$ evaluated at the same point is $F = 4.89 \pm .11$, a non-gaussian value, as we expect. A single filament, most of which is contained within a box of size $\sim N^{1/2}$, does not represent homogeneous turbulence, and thus it is not clear that one should compare this value to the value ~ 3.4 in homogeneous turbulence [2]. In a wake F takes values between 3 and 4.5 [20].

With values of N within our computational grasp (see the discussion below) it was not possible to evaluate velocity differences $u(\underline{x}) - u(\underline{x}')$ for $|\underline{x} - \underline{x}'|$ large enough to have

$u(\underline{x}), u(\underline{x}')$ independent and yet have both \underline{x} and \underline{x}' within a region with a substantial number of segments, thus the decay of the flatness of the velocity differences as the distance $|\underline{x} - \underline{x}'|$ increases cannot be compared with what happens in experiments. The correlation tensor has the correct qualitative form, but as explained in [2], this is mostly a consequence of $\text{div } \underline{u} = 0$ and sheds little light on the model.

(b) **Self-avoiding filaments.** These are generated by the pivot algorithm. The values of μ converge rapidly (for a detailed analysis, see [25]). With $N \geq 500$, $n > 10^4$, the estimates of μ are within 1% of the Flory value $\mu = 0.6$, with error estimates under 1%. The corresponding dimension is $D = 1.66$. The skewness S of $\partial u / \partial x$ is also zero with great accuracy.

In tables I and II we display computed values of μ' and F for several moderate values of N and n . The first N configurations are discarded to reduce the dependence on the initial configuration. The error estimates are calculated as if the successive realizations were independent. They are thus underestimates, but should not be catastrophically off since the acceptance rate of the pivot algorithm at these values of N is around 50% (i.e., about 50% of the proposed foldings turn out to be self-avoiding and are accepted); this value is consistent with the estimates in [25]. Furthermore, the moves in the pivot algorithm are quite radical, and thus independence of successive realization should not be far from being an acceptable supposition. A careful analysis of critical slow-down as $N \rightarrow \infty$ has turned out to be impractical because of the slow convergence.

From table III it appears that μ' converges to ~ 2.5 , and thus γ converges to ~ 0.4 . This is a key result in the present paper. The value 0.4 is intermediate between 0 and the no-intermittency value (here, $\gamma = 1$), just like the Kolmogorov exponent. The calculation shows that an inertial exponent can be generated by a non-local constraint, and under the assumption of thermal equilibrium. F , the flatness, converges more slowly, but remains above the gaussian value $F = 3$, as can be seen from table IV.

(c) **Constrained random walks.** This is of course the main model; it contains an additional parameter, the “temperature” T , which we would like to choose as small as possible in order to enforce the constraint of energy conservation, as discussed before. If T is too small the acceptance ratio, i.e., the fraction of moves in the weighted pivot algorithm

Table I μ' as a function of N and n for a self-avoiding filament ($\gamma = 1/\mu'$).

$n \backslash N$	401	501	601	701	801
10^4	2.96 ± 0.25	1.83 ± 0.06	2.04 ± 0.24	3.19 ± 0.49	4.75 ± 0.63
$5 \cdot 10^4$	2.65 ± 0.15	2.67 ± 0.10	2.34 ± 0.18	2.74 ± 0.36	2.95 ± 0.40
10^5	2.76 ± 0.16	2.44 ± 0.06	2.63 ± 0.20	2.54 ± 0.39	2.90 ± 0.33
$2 \cdot 10^5$	2.56 ± 0.12	2.53 ± 0.03	2.78 ± 0.18		

Table II

The flatness F as a function of N and n for a self-avoiding filament.

$n \backslash N$	501	601	701	801
10^4	3.51 ± 0.14	5.90 ± 0.18	3.71 ± 0.12	4.11 ± 0.16
$5 \cdot 10^4$	4.28 ± 0.08	6.02 ± 0.13	6.11 ± 0.23	3.18 ± 0.05
10^5	4.66 ± 0.06	5.98 ± 0.10	5.67 ± 0.14	3.81 ± 0.05

Table III

$D = 1/\mu$ as a function of N and n for a constrained random walk, $T = 14$.

$n \setminus N$	501	701
10^4	2.45 ± 0.06	2.47 ± 0.04
$5 \cdot 10^4$	2.36 ± 0.02	2.44 ± 0.02
10^5	2.33 ± 0.01	2.44 ± 0.02

Table IV

The flatness F as a function of N and n for a constrained random walk, $T = 14$.

$n \setminus N$	501	701
10^4	1.96 ± 0.36	2.27
$5 \cdot 10^4$	3.71 ± 0.5	6.41 ± 2.6
10^5	3.76 ± 0.4	5.26 ± 0.7

that is accepted, becomes very small and the results are not significant.

The exponent μ that determines the dimension $D = 1/\mu$ converges reasonably well. In table III we display values of D obtained with $T = 14$ and various choices of N and n . The error estimates are obtained from (9), where the uncertainty is estimated as 10 times the standard deviation, a plausible estimate since the acceptance ratio is 15%. It is reasonable to conclude that D at this value of T is around 2.5; if one disregards the difference in definition, this conclusion agrees with earlier determinations of related dimensions [6],[7],[8]. The runs summarized in table III are as large as we can afford; remember that the calculation of the energy E is $O(N^2)$, and at these values of N fast summation methods are not very helpful. The slightly larger values of D for a larger N may be a consequence of the fact that a fixed T produces a more severe constraint for a larger filament (with a larger set of possible values of E). In table IV we display some computed values of the flatness which are consistent with the runs previously described. The skewness is, as before, near zero. In all the calculations, the first $5N$ configurations are discarded.

It is important to examine the dependence of μ and D on the "temperature" T . For $T = 10$, $N = 501$, $n = 10^4$ we found $D = 2.58$, with an acceptance ratio of 9%, which makes the uncertainty large. Longer runs with the same values of T and N have a steadily decreasing acceptance ratio. With larger values of N and $T = 10$ the acceptance ratio tends to zero—the configurations get stuck at a fixed point. On the other hand, for $T > 15$ the calculated values of D decrease—at $T = 21$ they remain just above 2. Thus $T = 14$ seems to be the smallest practical value.

In none of the cases do we display the energy E . In the free case the energy should be near zero, in the self-avoiding case it should be positive, and in the constrained case it should be smaller than in the self-avoiding case. All these expectations are fulfilled, but the values of E depend on N , and we have not been able to find a convincing scaling that will clearly present the dominant trends.

One of the most interesting quantities is of course $\gamma = 1/\mu'$; unfortunately, the calculation of μ' does not converge as a function of N for the values of N we can afford. A calculation with $N = 701$, $n = 10^5$ costs about 10 hours of Cray XMP time, and at

$N = 701$ we are very far from convergence. The reason is clear; if $D = 2.5$, then $r_N \sim N^{0.4}$; even with $N = 1000$ most of the segments are within a sphere of radius less than 10—too close to the scale on which the folds are forming to distinguish the large scale structure of the vorticity field which we conjecture is dominated by the constraint of self-avoidance. In particular, with $N = 501$, $T = 14$, $n = 10^5$. $\langle \phi_N \rangle$ is negative, presumably as a result of the folds; with $N = 701$, $T = 14$, $n = 10^5$, $\langle \phi_N \rangle$ is positive, with μ' calculated as -2.36 ± 0.37

To show the qualitative effects of self-avoidance and energy conservation, we display in figures 1 and 2 some typical configurations. In figure 1 we display the first 100 links in a self-avoiding walk with $N = 501$, after $n = 10^4$ steps. In figure 2 we display the first 200 links in a constrained walk, with $T = 14$, after $n = 10^4$ steps with $N = 501$. The energy constraint creates tangles which presumably simply avoid each other in the large, since there should be no energy gain or loss in getting complicated tangles close to each other.

Conclusions

The model described above is a simplified version of a model of the inertial range in which the flow is dominated by vortex filaments in thermal equilibrium. The model has similarities to a polymer system for which it is known that a critical point is approached as the number of links N tends to infinity. Since vortex filaments become longer and thinner as the viscosity tends to zero, this analogy gives a concrete content to the conjecture that a turbulent flow approaches a critical state as the viscosity tends to zero, as is suggested by the strong coupling between scales. The Biot-Savart law that produces a velocity field from the filamentary vorticity produces non-gaussian velocity statistics.

The Hausdorff dimension D of the support of the vorticity produced by the model is near 2.5, in agreement with the values of D calculated in earlier work. The difference in the definition of D should be noted.

For a self-avoiding filament model there is an inertial range exponent, with a value that corresponds to an intermittent flow. This observation shows how an inertial range can be produced by global constraints in an equilibrium model. The conjecture that such an exponent is also produced in the constrained filament model could not be verified because of limitations in computing power. One could argue that in spectral calculations (see e.g.

[31]) one tries to stay as far as possible from the critical point $\nu = 0$ ($\nu \equiv$ viscosity) while still having an inertial range, a strategy that is difficult to follow with vortex methods or vortex models. The calculations here should make one wary of all numerical determinations of Kolmogorov's exponent. Calculations of that exponent based on vortex methods must take the vortex cores into account.

The model lends support to the idea that in vortex calculations the folds ("hairpins") can be removed in a systematic way. A first attempt to carry out such a removal is described in [12]. A more systematic attempt that makes use of a phenomenological Hamiltonian of the form (8) will be described elsewhere.

Note: the programs used to perform the calculations above are available from the author.

References

1. C. Anderson and C. Greengard, Vortex methods, Lecture notes in mathematics, Springer, vol. 1360, 1988.
2. G. Batchelor, The theory of homogeneous turbulence, Cambridge University Press, 1960.
3. T. Beale and A. Majda, Vortex methods I: Convergence in three dimensions, Math. Comp., 39, 1-27 (1982).
4. T. Beale and A. Majda, Vortex methods II: Higher order accuracy in two and three space dimensions, Math. Comp., 32, 29-52 (1982).
5. K. Binder (ed.), Applications of the Monte-Carlo method in statistical physics, Topics in current physics, Springer, vol. 36, 1984.
6. A.J. Chorin, Estimates of intermittency, spectra and blow-up in fully developed turbulence, Comm. Pure Appl. Math., 34, 853-866 (1981).
7. A.J. Chorin, The evolution of a turbulent vortex, Comm. Math. Phys., 83, 517-535 (1982).
8. A.J. Chorin, Turbulence and vortex stretching on a lattice, Comm. Pure Appl. Math., 39 (special issue), S47-S65 (1986).
9. A.J. Chorin, Lattice vortex models and turbulence theory, in 'Wave motion', Lax 60th birthday volume, A. Chorin and A. Majda (eds.), MSRI-Springer, 1987.
10. A.J. Chorin, Scaling laws in the lattice vortex model of turbulence, Comm. Math. Phys., 114, 167-176 (1988).
11. A.J. Chorin, Spectrum, dimension and polymer analogies in fluid turbulence, Phys. Rev. Lett., 60, 1947-1949 (1988).
12. A.J. Chorin, Hairpin removal in vortex interactions, LBL report LBL-26173, Lawrence Berkeley Laboratory, 1988.
13. A.J. Chorin, Vortices, turbulence, and statistical mechanics, to appear in "Vortex Methods", K. Gustafson and J. Sethian (editors), SIAM publication, 1989.
14. A.J. Chorin and J. Marsden, A mathematical introduction to fluid mechanics, Springer, 1979.
15. D. Foster, Hydrodynamic fluctuations, broken symmetry and correlation functions, Frontiers in physics, Benjamin, 1975.
16. O. Frostman, Potentiel d'équilibre et théorie des ensembles, Thesis, Lund, 1935.
17. P.G. de Gennes, Scaling concepts in polymer physics, Cornell University Press, 1971.
18. O.H. Hald, Convergence of vortex methods II, SIAM J. Sc. Stat. Comp., 16, 726-755 (1979).
19. O.H. Hald, Smoothness properties of the Euler flow map, manuscript, 1987.
20. J.O. Hinze, Turbulence, Mc-Graw-Hill, 1975.
21. O. Knio and A. Ghoniem, Three dimensional vortex methods, J. Comp. Phys, in press.
22. M. Lal, Monte-Carlo computer simulations of chain molecules, Molecular physics, 17, 57-64 (1969).
23. H. Lamb, Hydrodynamics, Dover, NY, 1932.
24. S.K. Ma, Modern theory of critical phenomena, Benjamin, Boston, 1976.
25. N. Madras and A. Sokal, The pivot algorithm: a highly efficient Monte-Carlo method for self-avoiding walks, J. Stat. Phys., 50, 109-186 (1988).

26. H.K. Moffatt, On the degree of knottedness of tangled vortex lines, *J. Fluid Mech.*, 35, 117-132 (1969).
27. G. Papanicolaou, D. Stroock, and S.R.S. Varadhan, A martingale approach to some limit theorems, in "Statistical mechanics and dynamical systems", Duke Turbulence Conference, D. Ruelle (ed.), Duke University Series, vol. 3, 1977.
28. D. Revuz and M. Yor, Continuous martingale calculus, Chap. 13, Springer, 1989.
29. M. Rogers and P. Moin, The structure of the vorticity field in homogeneous turbulent flows, *J. Fluid Mech.*, 176, 33-66 (1987).
30. K.J.R. Sreenivasan and C. Meneveau, The fractal aspects of turbulence, *J. Fluid Mech.*, 173, 357-386 (1986).
31. K. Yamamoto and I. Hosokawa, A decaying isotropic turbulence pursued by the spectral method, *J. Phys. Soc. Japan*, 57, 1532-1535 (1988).

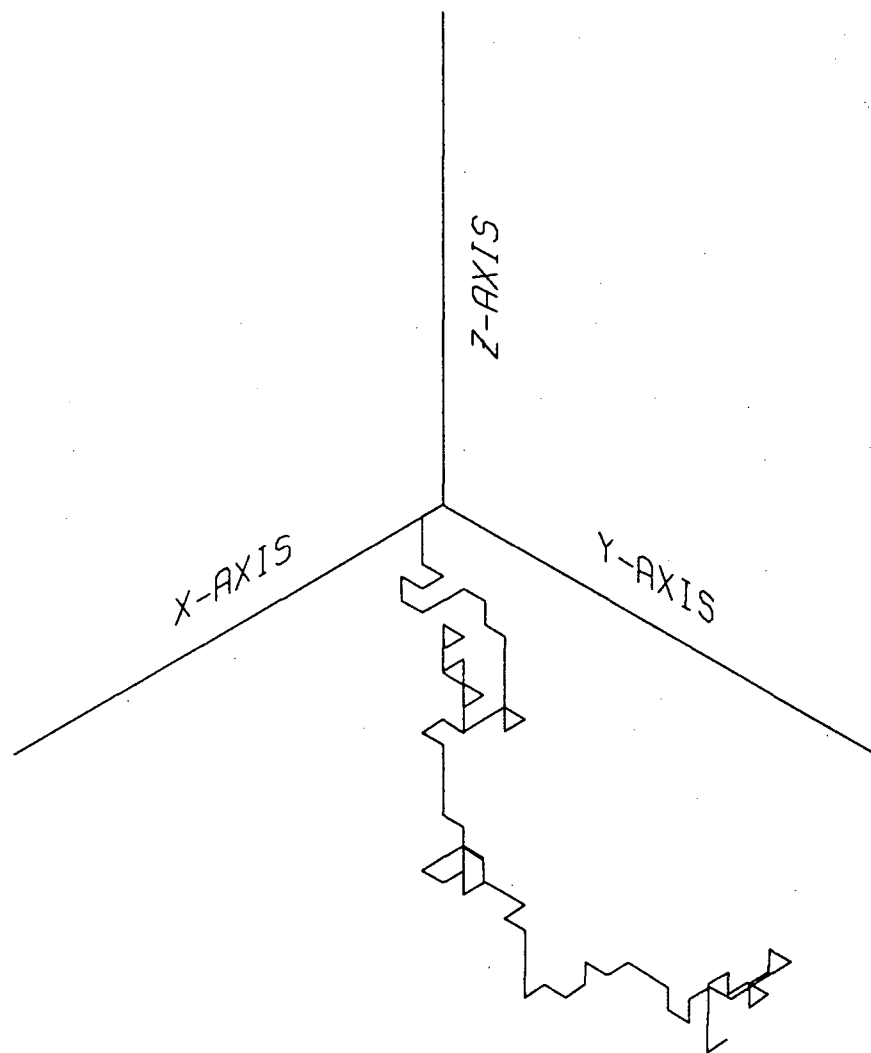


Fig. 1. A self avoiding walk.

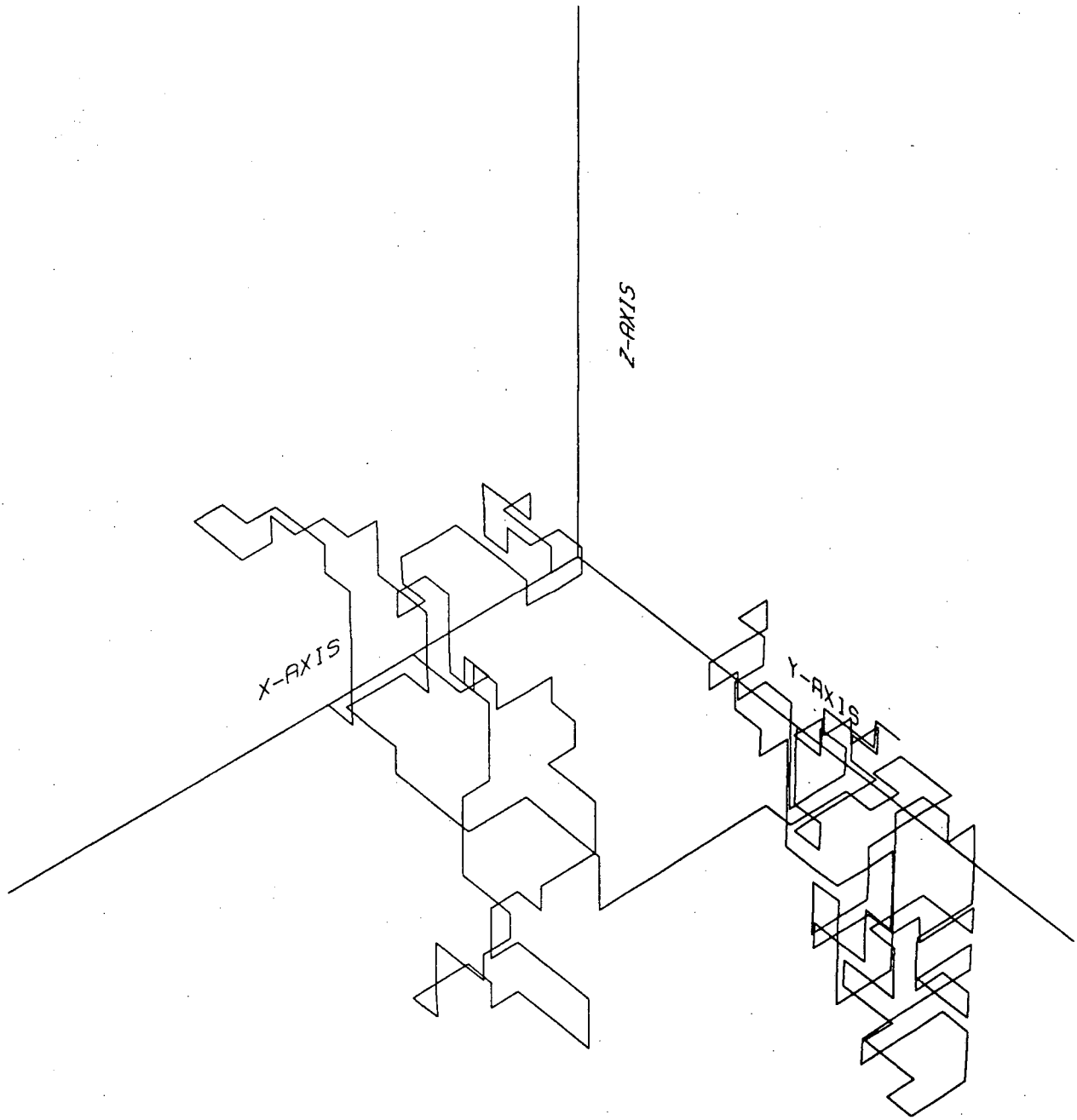


Fig. 2. A constrained random walk.

LAWRENCE BERKELEY LABORATORY
TECHNICAL INFORMATION DEPARTMENT
1 CYCLOTRON ROAD
BERKELEY, CALIFORNIA 94720